Precise Determination of the Electric and Magnetic Form Factors of the Proton

Michael O. Distler for the A1 collaboration @ MAMI

Institut für Kernphysik
Johannes Gutenberg-Universität Mainz

The Structure and Dynamics of Hadrons
International Workshop XXXIX on Gross Properties of Nuclei and Nuclear Excitations
Hirschegg, Kleinwalsertal, Austria, January 21, 2011

Outline

Introduction I: The size of the proton

Nature **466**, 213-216 (8 July 2010)

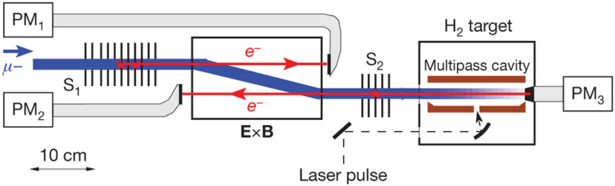

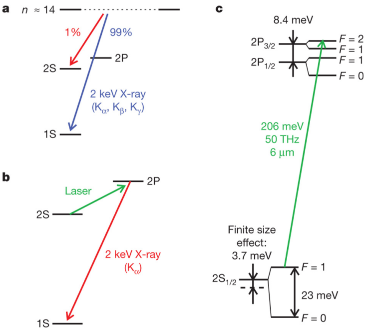

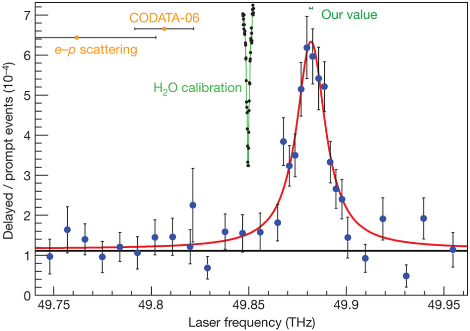

Cross section and form factors for elastic e-p scattering

The cross section:

$$\frac{\left(\frac{d\sigma}{d\Omega}\right)}{\left(\frac{d\sigma}{d\Omega}\right)_{Mott}} = \frac{1}{\varepsilon\,(1+\tau)}\left[\varepsilon G_E^2\left(Q^2\right) + \tau G_M^2\left(Q^2\right)\right]$$

with:

$$\tau = \frac{Q^2}{4m_p^2}, \quad \varepsilon = \left(1 + 2\,(1+\tau)\tan^2\frac{\theta_e}{2}\right)^{-1}$$

Fourier-transform of $G_E,\ G_M \rightarrow$ spatial distribution (Breit frame)

$$\left\langle r_E^2\right\rangle = -6\hbar^2\,\frac{\mathrm{d}G_E}{\mathrm{d}Q^2}\bigg|_{Q^2=0} \qquad \left\langle r_M^2\right\rangle = -6\hbar^2\,\frac{\mathrm{d}\left(G_M/\mu_p\right)}{\mathrm{d}Q^2}\bigg|_{Q^2=0}$$

Overview of different proton charge-radius results

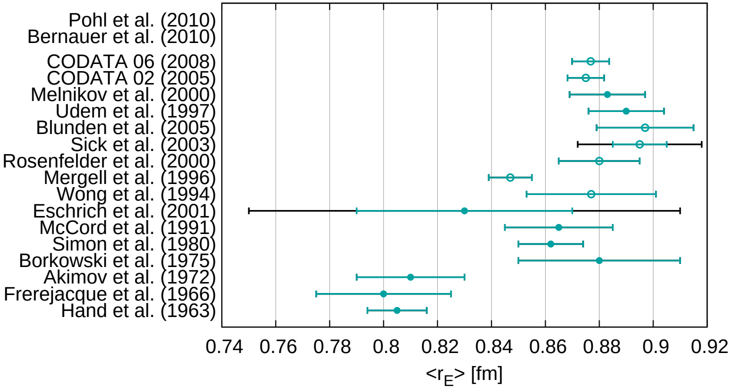

Filled dots: Results from new measurements.
Hollow dots: Reanalysis of existing data.

Overview of different proton charge-radius results

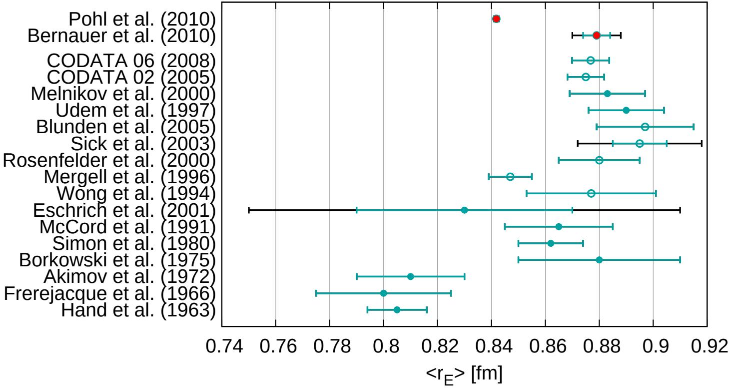

Filled dots: Results from new measurements.
Hollow dots: Reanalysis of existing data.

Introduction II: Original Motivation

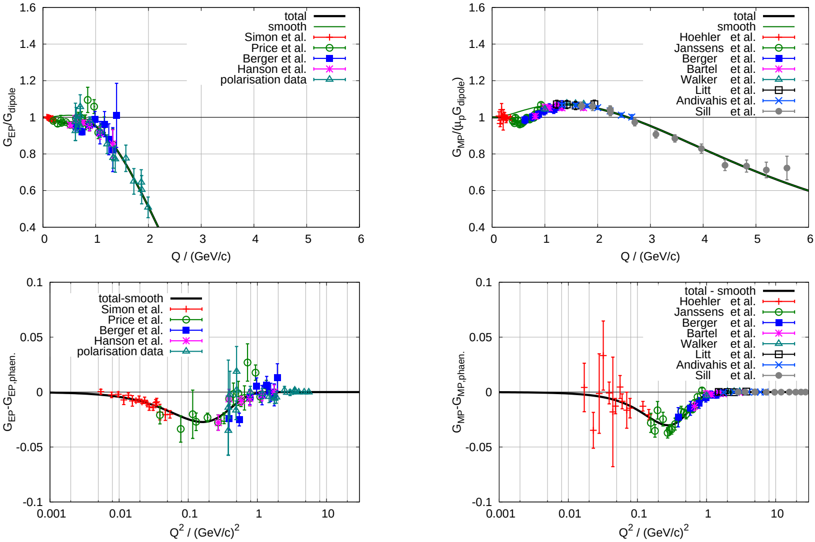

(see J. Friedrich and Th. Walcher, Eur. Phys. J. A **17** (2003) 607)

Introduction II: Original Motivation

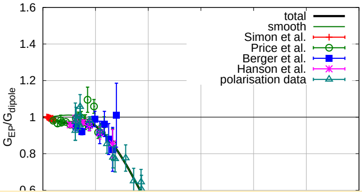

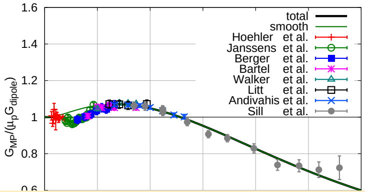

Discrepancy of existing values for proton electric radius:

- 0.809(11) fm: standard dipole at HEPL (Hand et al. 1963)
- 0.862(12) fm: low Q^2 at Mainz (Simon et al. 1979)
- 0.847(09) fm: dispersion relation (Mergell et al. 1996)
- 0.890(14) fm: Hydrogen Lamb shift (Udem et al. 1997)

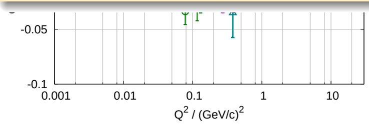

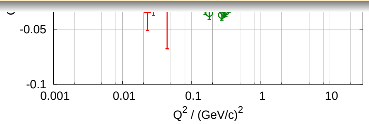

(see J. Friedrich and Th. Walcher, Eur. Phys. J. A **17** (2003) 607)

The Mainz Microtron MAMI

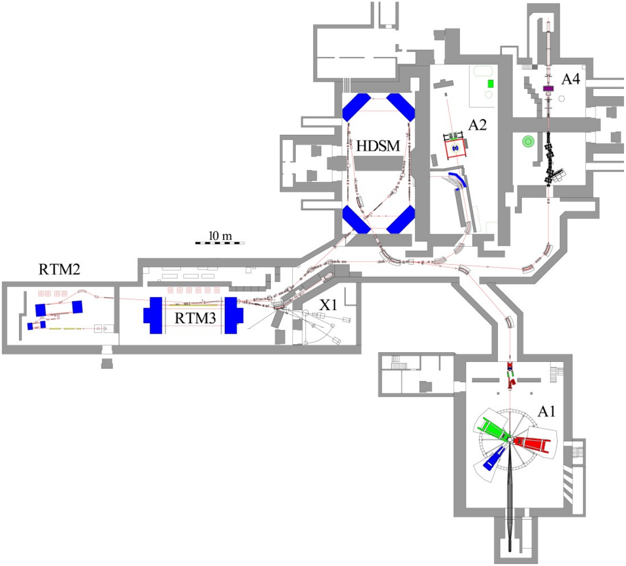

The Mainz Microtron MAMI

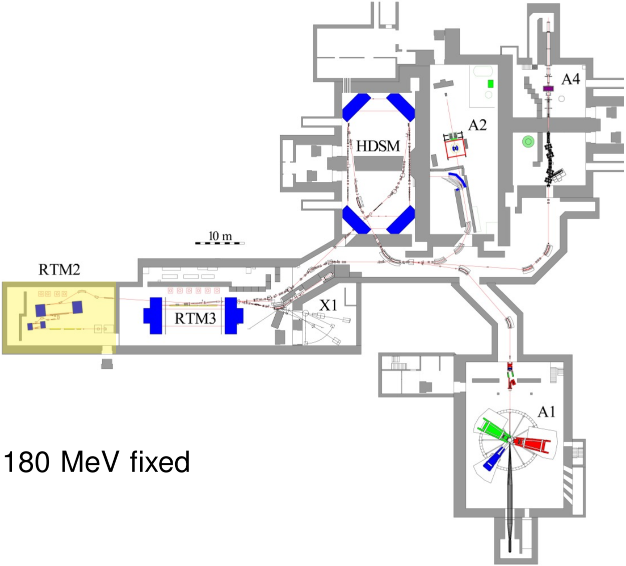

- MAMI-A: 180 MeV fixed

The Mainz Microtron MAMI

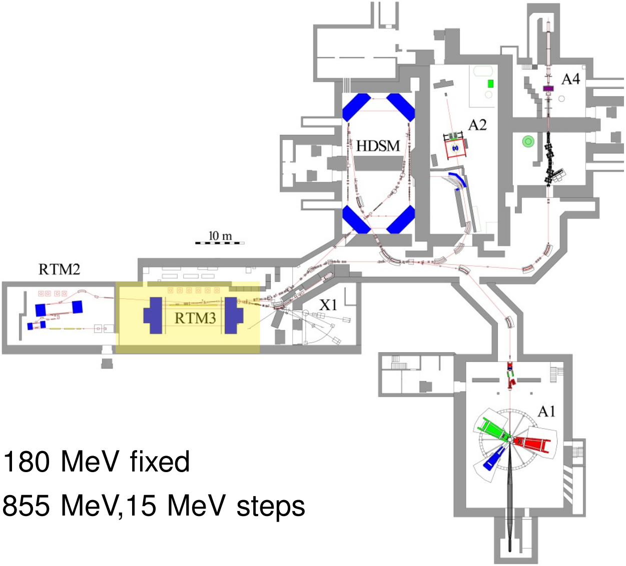

- MAMI-A: 180 MeV fixed
- MAMI-B: 855 MeV,15 MeV steps

The Mainz Microtron MAMI

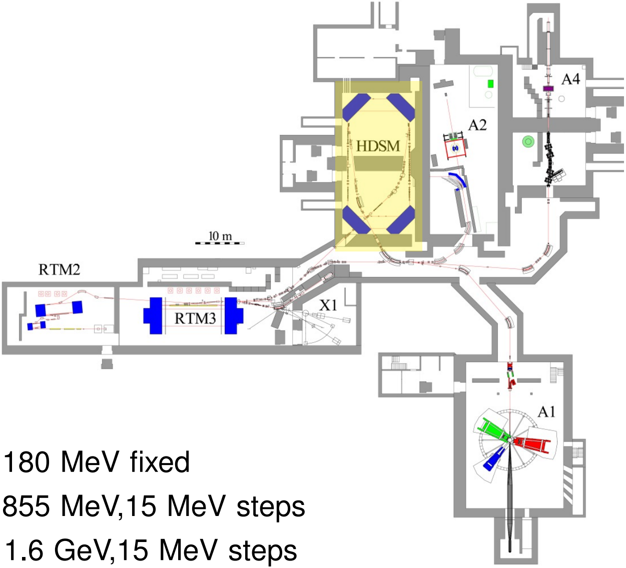

- MAMI-A: 180 MeV fixed
- MAMI-B: 855 MeV,15 MeV steps
- MAMI-C: 1.6 GeV,15 MeV steps

The Mainz Microtron MAMI

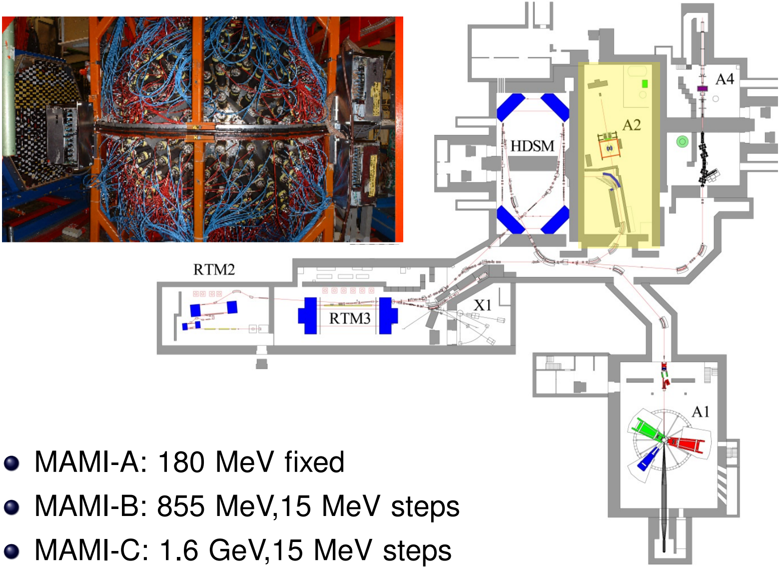

- MAMI-A: 180 MeV fixed
- MAMI-B: 855 MeV,15 MeV steps
- MAMI-C: 1.6 GeV,15 MeV steps

The Mainz Microtron MAMI

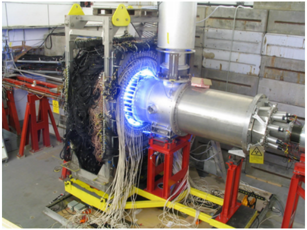

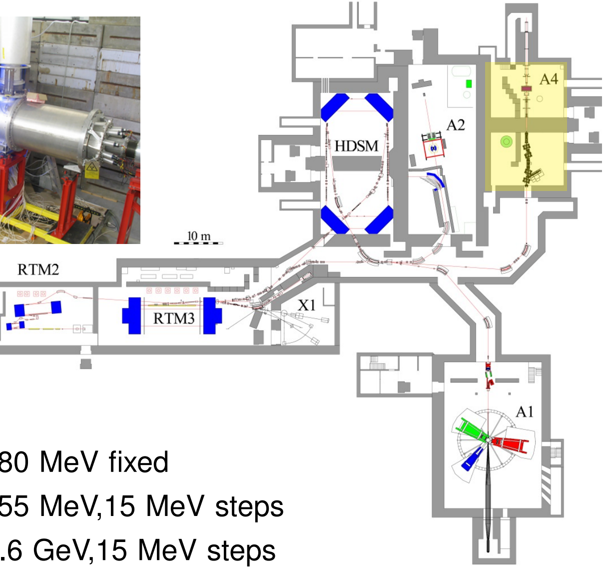

- MAMI-A: 180 MeV fixed
- MAMI-B: 855 MeV,15 MeV steps
- MAMI-C: 1.6 GeV,15 MeV steps

The Mainz Microtron MAMI

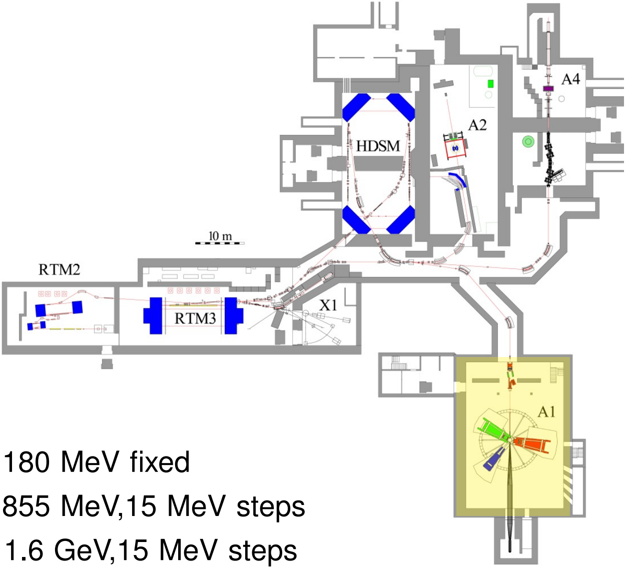

- MAMI-A: 180 MeV fixed
- MAMI-B: 855 MeV,15 MeV steps
- MAMI-C: 1.6 GeV,15 MeV steps

The Mainz high-precision p(e,e')p measurement: Three spectrometer facility of the A1 collaboration

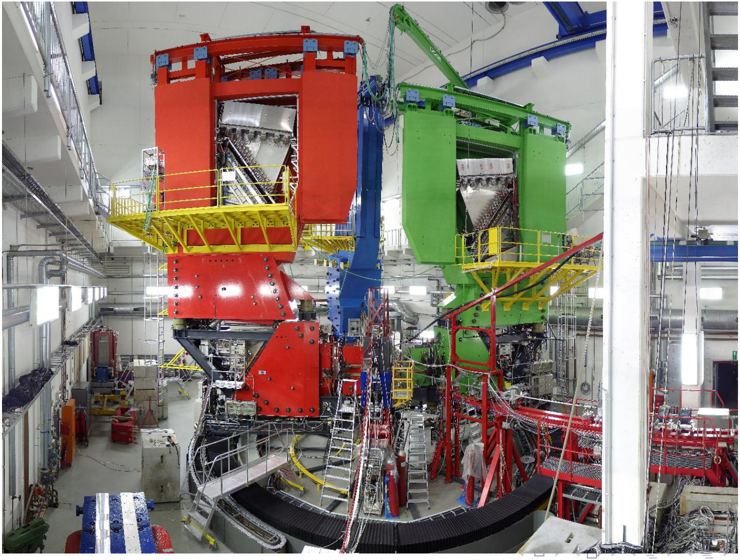

Design goal: High precision

- Statistical precision: 20 min beam time for <0.1%

Design goal: High precision through redundancy

- Statistical precision: 20 min beam time for <0.1%
- Control of luminosity and systematic errors:
  Measure all quantities in as many ways as possible:

Design goal: High precision through redundancy

- Statistical precision: 20 min beam time for <0.1%
- Control of luminosity and systematic errors:
  Measure all quantities in as many ways as possible:
  - Beam current:
    Foerster probe (usual way) $\Longleftrightarrow$ pA-meter
    $\longrightarrow$ measures down to extremely low currents for small θ

Design goal: High precision through redundancy

- Statistical precision: 20 min beam time for <0.1%
- Control of luminosity and systematic errors:
  Measure all quantities in as many ways as possible:
  - Beam current:
    Foerster probe (usual way) $\Longleftrightarrow$ pA-meter
    $\longrightarrow$ measures down to extremely low currents for small θ
  - Luminosity:
    current $\times$ density $\times$ target length
    $\Longleftrightarrow$ third magnetic spectrometer as monitor

Design goal: High precision through redundancy

- Statistical precision: 20 min beam time for <0.1%
- Control of luminosity and systematic errors:
  Measure all quantities in as many ways as possible:
  - Beam current:
    Foerster probe (usual way) $\Longleftrightarrow$ pA-meter
    $\longrightarrow$ measures down to extremely low currents for small θ
  - Luminosity:
    current $\times$ density $\times$ target length
    $\Longleftrightarrow$ third magnetic spectrometer as monitor
  - Overlapping acceptance
  - Where possible: Measure at the same scattering angle with two spectrometers

Measured settings and future (high Q^2) expansion

$$\frac{d\sigma}{d\Omega} = \left(\frac{d\sigma}{d\Omega}\right)_{Mott} \frac{1}{\varepsilon(1+\tau)} \left[\varepsilon G_E^2\left(Q^2\right) + \tau G_M^2\left(Q^2\right)\right]$$

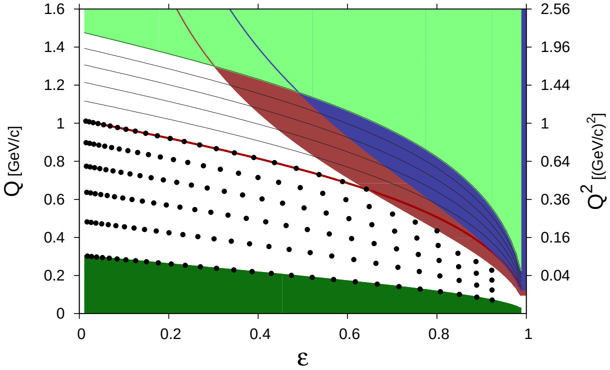

spectrometer A limit
spectrometer B limit
MAMI min. E= 180 MeV
MAMI-C max. E=1.53 GeV
MAMI-B max. E= 855 MeV

Measured settings and future (high Q^2) expansion

$$\frac{d\sigma}{d\Omega} = \left(\frac{d\sigma}{d\Omega}\right)_{Mott} \frac{1}{\varepsilon(1+\tau)} \left[\varepsilon G_E^2\left(Q^2\right) + \tau G_M^2\left(Q^2\right)\right]$$

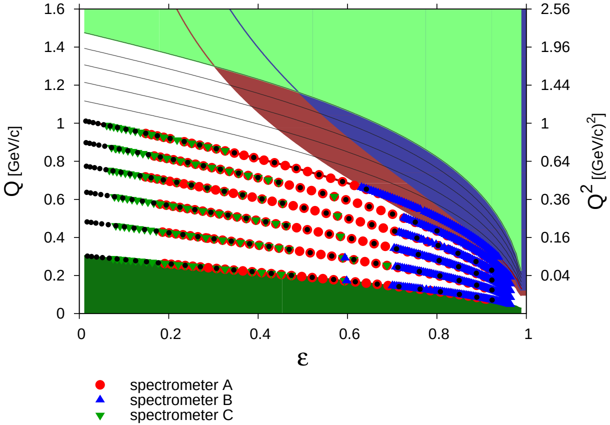

- ∼90 GByte on disc
- ∼1400 Settings
- $> 10^9$ events.

Background

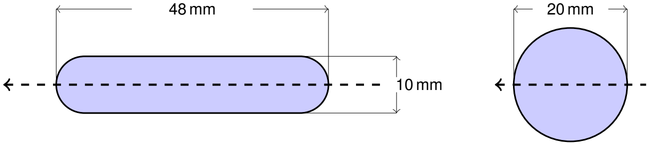

Background

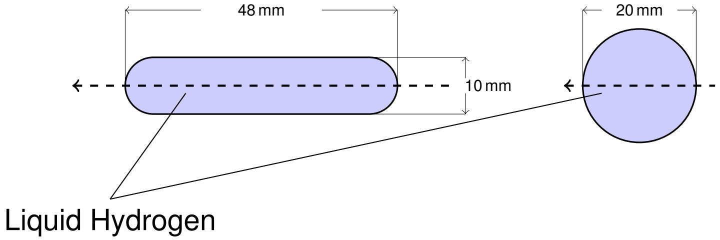

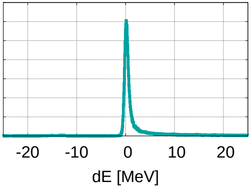

Background

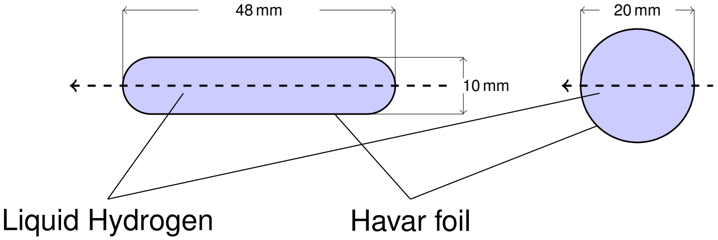

48 mm
20 mm
10 mm
Liquid Hydrogen
Havar foil

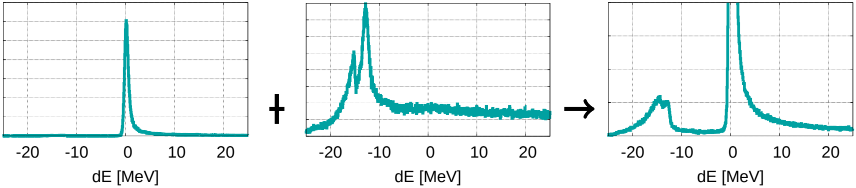

-20
-10
0
10
20
dE [MeV]
+
-20
-10
0
10
20
dE [MeV]
→
-20
-10
0
10
20
dE [MeV]

Simulation:

- Model for energy loss and small angle scattering
- Input: momentum-, angular-, vertex resolution

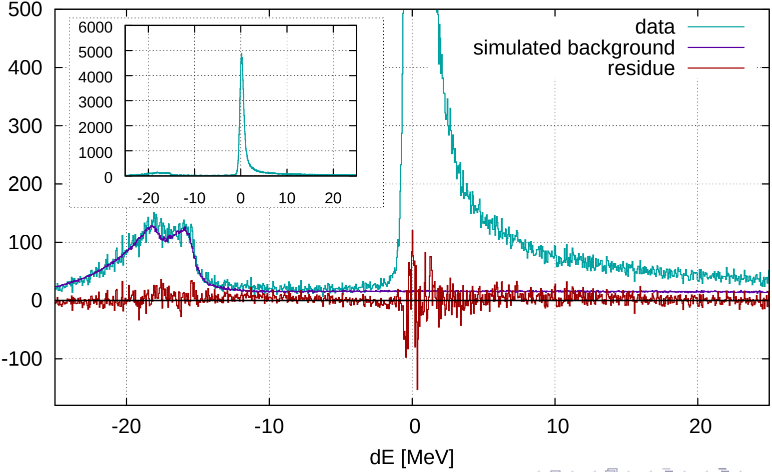

Feynman graphs of leading and next to leading order for elastic scattering

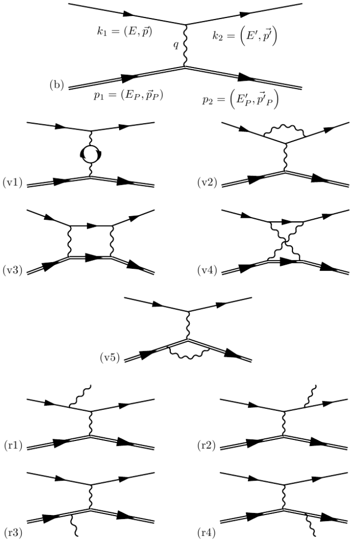

All graphs are taken into account:

- vacuum polarization (v1): e, (μ, τ) *Maximon/Tjon (2000) and Vanderhaeghen et al. (2000)*
- electron vertex correction
- Coulomb distortion (two photon exchange)
- real photon emission

Description of the radiative tail

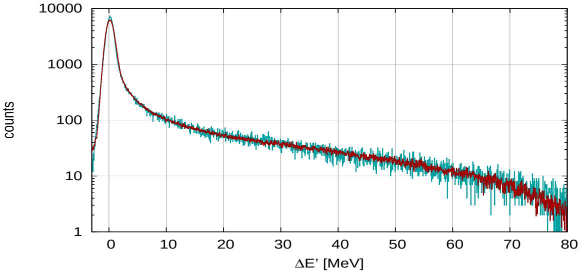

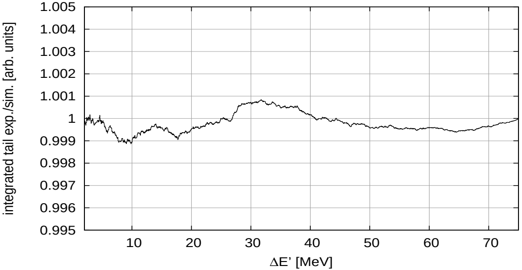

Cross sections

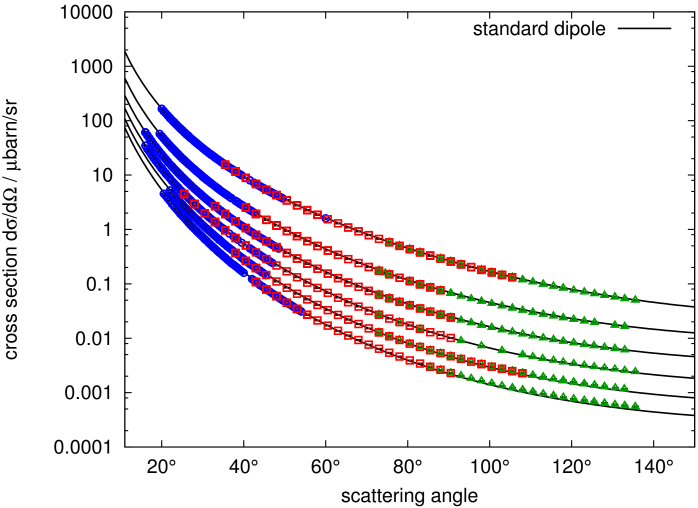

Cross sections / standard dipole

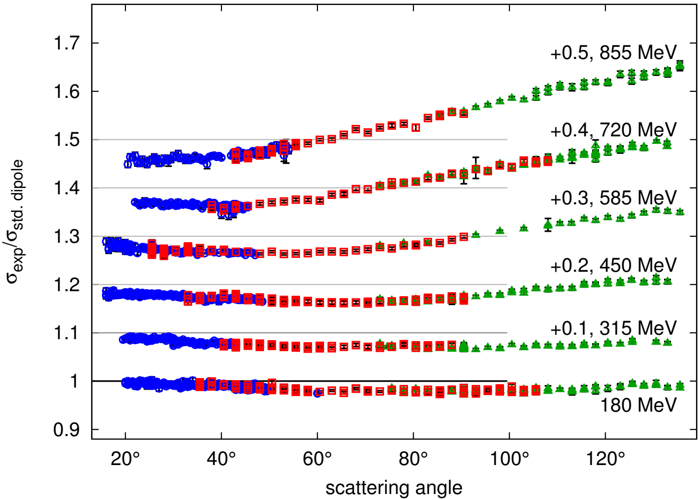

How to extract the form factors?

Two methods:

1. Classical Rosenbluth separation

How to extract the form factors?

Two methods:

1. Classical Rosenbluth separation
2. ”Super-Rosenbluth separation”: Fit of form factor models directly to the measured cross sections
   - Feasible due to fast computers.
   - All data at all Q^2 and ε values contribute to the fit, i.e. full kinematical region used, no projection (to specific Q^2) needed.
   - Easy fixing of normalization.

How to extract the form factors?

Two methods:

1. Classical Rosenbluth separation
2. ”Super-Rosenbluth separation”: Fit of form factor models directly to the measured cross sections
   - Feasible due to fast computers.
   - All data at all Q^2 and ε values contribute to the fit, i.e. full kinematical region used, no projection (to specific Q^2) needed.
   - Easy fixing of normalization.
   - Model dependence?

How to extract the form factors?

Two methods:

1. Classical Rosenbluth separation
2. ”Super-Rosenbluth separation”: Fit of form factor models directly to the measured cross sections
   - Feasible due to fast computers.
   - All data at all Q^2 and ε values contribute to the fit, i.e. full kinematical region used, no projection (to specific Q^2) needed.
   - Easy fixing of normalization.
   - Model dependence?

For radii extraction: Needs a fit anyway!
Classical Rosenbluth: Extracted G_E and G_M highly correlated!
$\Longrightarrow$Error propagation very involved.

Models: Dipols

Dipole (different b for G_E and G_M):

$$G_D\left(Q^2, b\right) = \frac{1}{\left(1 + \frac{Q^2}{b}\right)^2}$$

Double Dipole (as in Friedrich/Walcher phenomenological fit [Eur. Phys. J. A **17** (2003) 607]):

$$G_{DD}\left(Q^2, a, b_1, b_2\right) = aG_D\left(Q^2, b_1\right) + (1 - a)\, G_D\left(Q^2, b_2\right)$$

Models: Polynomial

Polynomial

$$G_P\left(Q^2, a_1, \ldots, a_n\right) = 1 + \sum_{i=1}^{n} a_i Q^{2\cdot i}$$

Polynomial + standard Dipole

$$G_{PAD}\left(Q^2, a_1, \ldots, a_n\right) = G_D\left(Q^2, 0.71\right) + \sum_{i=1}^{n} a_i Q^{2\cdot i}$$

Polynomial × standard Dipole

$$G_{PMD}\left(Q^2, a_1, \ldots, a_n\right) = G_D\left(Q^2, 0.71\right) \cdot \left(1 + \sum_{i=1}^{n} a_i Q^{2\cdot i}\right)$$

Models: Splines

Uniform cubic splines

$$spline\left(Q^2, a_1, \ldots, a_n\right)$$

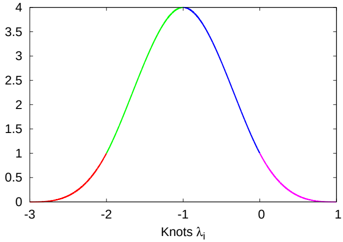

Spline:

$$G_{Spline}\left(Q^2, a_1, \ldots, a_n\right) = 1 + Q^2 \cdot spline\left(Q^2\right)$$

Spline $\times$ standard Dipole

$$G_{SMD}\left(Q^2, a_1, \ldots, a_n\right) = G_D\left(Q^2, 0.71\right) \cdot \left(1 + Q^2 \cdot spline\left(Q^2\right)\right)$$

Models: Misc

Also:

- Friedrich / Walcher phenomenological ansatz
- extended Gari-Krümpelmann (VMD), Lomon et al.
- Arrington type:

$$\frac{P^N}{P^{N+2}}$$

Cross sections / standard dipole

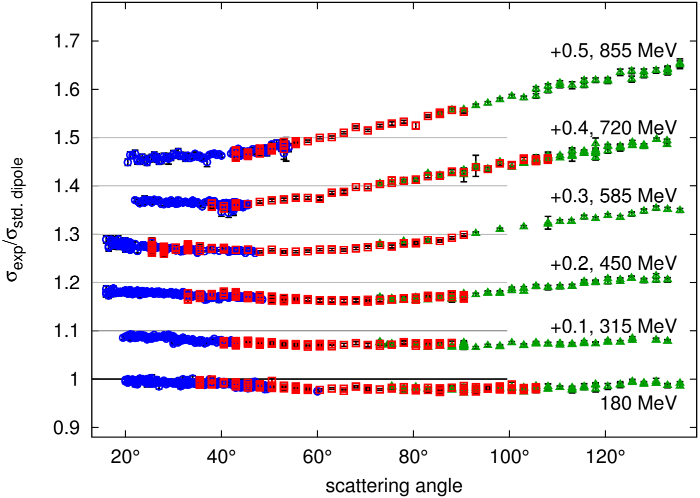

Cross sections + spline fit

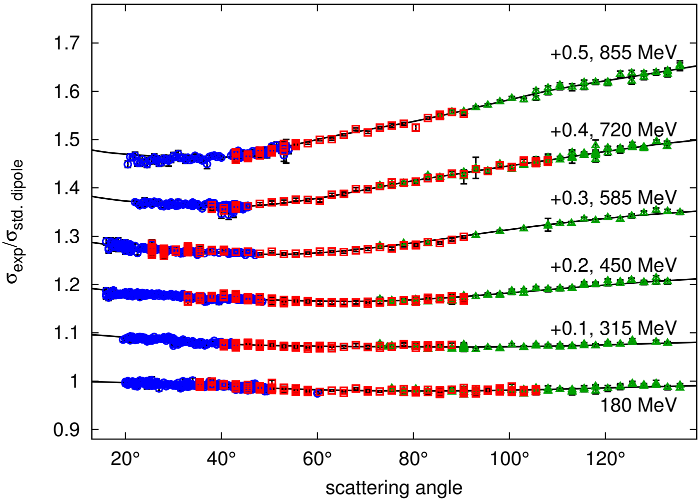

Cross sections: 180 MeV

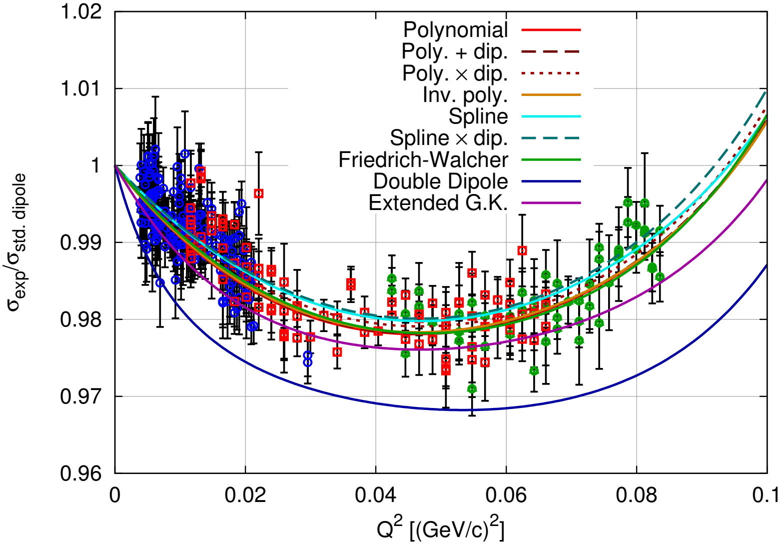

Form factor results

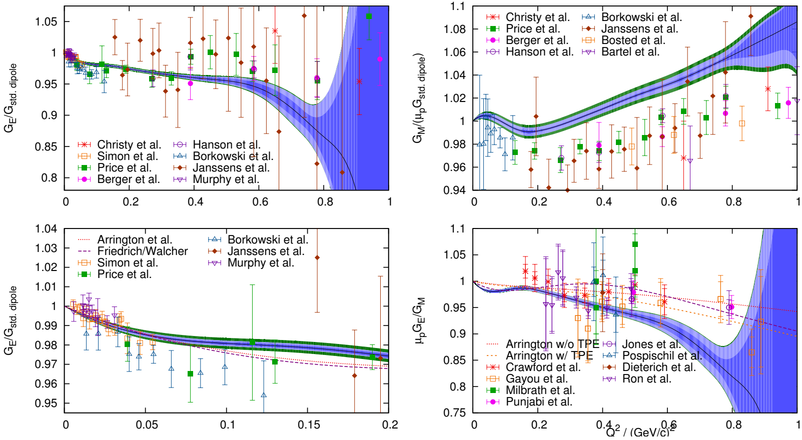

Jan C. Bernauer *et al.*, "High-precision determination of the electric and magnetic form factors of the proton", PRL 105, 242001 (2010), arXiv:1007.5076

The electric rms radius - extracted by different models

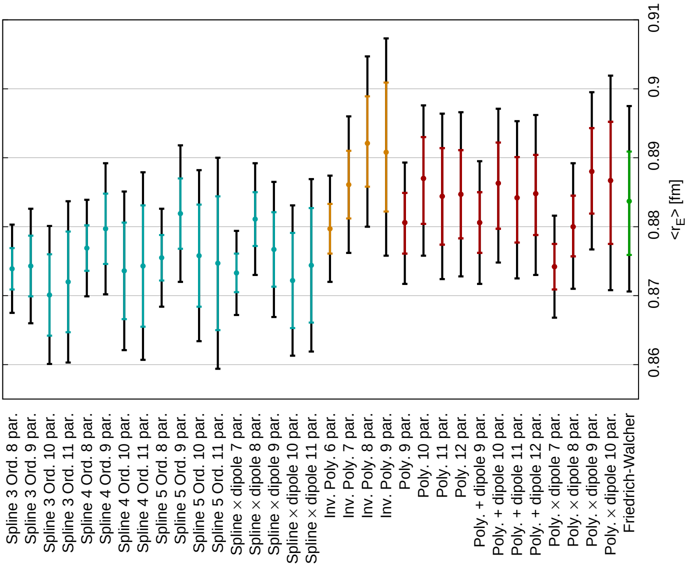

Conclusion – Part I

- High precision e-p scattering data from MAMI.
  PRL 105, 242001 (2010), arXiv:1007.5076.
- Q^2 range from 0.003 to 1 $(\mathrm{GeV/c})^2$.
- Consistent data set.
- "Super-Rosenbluth" fit to determine form factors and radii.
- The charge and magnetic rms radii are determined as

$$\begin{aligned}
\langle r_e \rangle &= 0.879 \pm 0.005_{\mathrm{stat.}} \pm 0.004_{\mathrm{syst.}} \pm 0.002_{\mathrm{model}} \pm 0.004_{\mathrm{group}}\ \mathrm{fm}, \\
\langle r_m \rangle &= 0.777 \pm 0.013_{\mathrm{stat.}} \pm 0.009_{\mathrm{syst.}} \pm 0.005_{\mathrm{model}} \pm 0.002_{\mathrm{group}}\ \mathrm{fm}.
\end{aligned}$$

Supported by the "Deutsche Forschungsgemeinschaft (DFG)" with a "Sonderforschungsbereich (SFB443)".

Outlook

- Jan Bernauer joined the
  OLYMPUS Experiment @ DESY/Hamburg
  (Spokesperson: Richard Milner, MIT)
- OLYMPUS: Determine the effect of two-photon exchange in elastic lepton-proton scattering by precisely measuring the ratio of positron-proton
  to electron-proton elastic unpolarized cross sections.
- low Q^2 extension: ISR @ MAMI
- MAMI: Form factors and polarizability of D and $^{3,4}He$
  PSI: Lamb shift in myonic deuterium and myonic helium.

Discussion of the Lamb shift / electron scattering discrepancy

The following tables are taken from the 'QED supplement' published in *Nature* **466**, 213-216 (8 July 2010).
'**All known radius-independent contributions**' and '**all relevant radius-dependent contributions**' to the Lamb shift in μp from different authors are listed.

2S – 2P splitting in muonic hydrogen

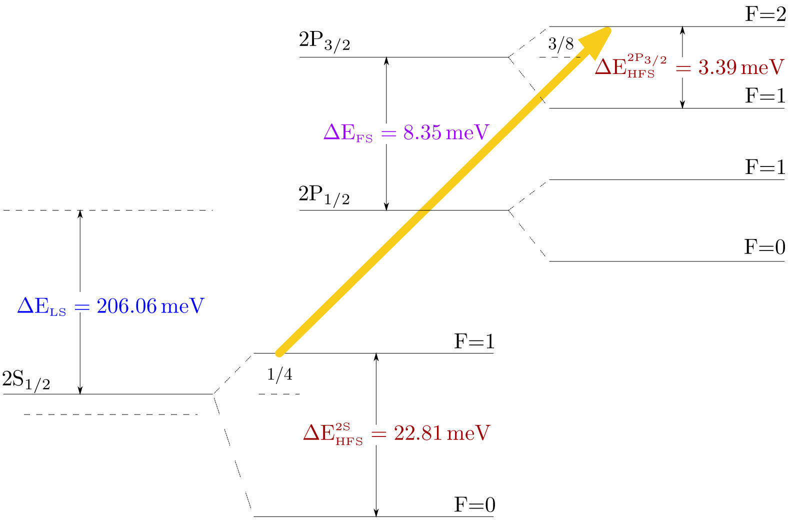

2S – 2P splitting in muonic hydrogen

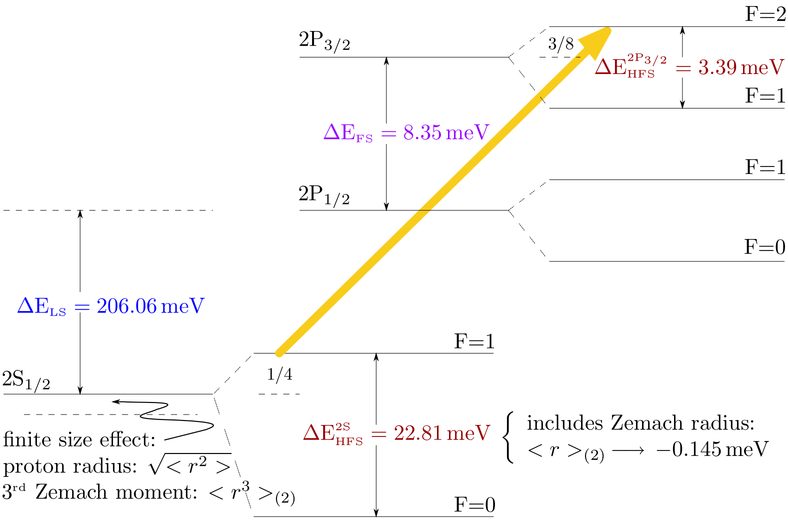

Discussion of the Lamb shift / electron scattering discrepancy

#	Contribution		Our selection		Pachucki[1–3]		Borie[5]	
		Ref.	Value	Unc.	Value	Unc.	Value	Unc.
1	NR One loop electron VP	1,2			205.0074			
2	Relativistic correction (corrected)	1–3,5			0.0169			
3	Relativistic one loop VP	5	205.0282				205.0282	
4	NR two-loop electron VP	5,14	1.5081		1.5079		1.5081	
5	Polarization insertion in two Coulomb lines	1,2,5	0.1509		0.1509		0.1510	
6	NR three-loop electron VP	11	0.00529					
7	Polarisation insertion in two and three Coulomb lines (corrected)	11,12	0.00223					
8	Three-loop VP (total, uncorrected)				0.0076		0.00761	
9	Wichmann-Kroll	5,15,16	−0.00103				−0.00103	
10	Light by light electron loop contribution (Virtual Delbrück scattering)	6	0.00135	0.00135			0.00135	0.00015
11	Radiative photon and electron polarization in the Coulomb line $\alpha^2(Z\alpha)^4$	1,2	−0.00500	0.0010	−0.006	0.001	−0.005	
12	Electron loop in the radiative photon of order $\alpha^2(Z\alpha)^4$	17–19	−0.00150					
13	Mixed electron and muon loops	20	0.00007				0.00007	
14	Hadronic polarization $\alpha(Z\alpha)^4 m_r$	21–23	0.01077	0.00038	0.0113	0.0003	0.011	0.002
15	Hadronic polarization $\alpha(Z\alpha)^5 m_r$	22,23	0.000047					
16	Hadronic polarization in the radiative photon $\alpha^2(Z\alpha)^4 m_r$	22,23	−0.000015					
17	Recoil contribution	24	0.05750		0.0575		0.0575	
18	Recoil finite size	5	0.01300	0.001			0.013	0.001
19	Recoil correction to VP	5	−0.00410				−0.0041	
20	Radiative corrections of order $\alpha^n(Z\alpha)^k m_r$	2,7	−0.66770		−0.6677		−0.66788	
21	Muon Lamb shift 4th order	5	−0.00169				−0.00169	
22	Recoil corrections of order $\alpha(Z\alpha)^5 \frac{m}{M} m_r$	2,5–7	−0.04497		−0.045		−0.04497	
23	Recoil of order α^6	2	0.00030		0.0003			
24	Radiative recoil corrections of order $\alpha(Z\alpha)^n \frac{m}{M} m_r$	1,2,7	−0.00960		−0.0099		−0.0096	
25	Nuclear structure correction of order $(Z\alpha)^5$ (Proton polarizability contribution)	2,5,22,25	0.015	0.004	0.012	0.002	0.015	0.004
26	Polarization operator induced correction to nuclear polarizability $\alpha(Z\alpha)^5 m_r$	23	0.00019					
27	Radiative photon induced correction to nuclear polarizability $\alpha(Z\alpha)^5 m_r$	23	−0.00001					
	Sum		206.0573	0.0045	206.0432	0.0023	206.05856	0.0046

Discussion of the Lamb shift / electron scattering discrepancy

$$\Delta E = 209.9779(49) - 5.2262\, r_p^2 + 0.0347\, r_p^3$$

Values are in meV and radii in fm.

Contribution	Ref.	our selection		Pachucki[2]	Borie[5]
Leading nuclear size contribution	[26]	−5.19745	$< r_p^2 >$	−5.1974	−5.1971
Radiative corrections to nuclear finite size effect	[2,26]	−0.0275	$< r_p^2 >$	−0.0282	−0.0273
Nuclear size correction of order $(Z\alpha)^6 < r_p^2 >$	[1,27–29]	−0.001243	$< r_p^2 >$		
Total $< r_p^2 >$ contribution		−5.22619	$< r_p^2 >$	−5.2256	−5.2244
Nuclear size correction of order $(Z\alpha)^5$	[1,2]	0.0347	$< r_p^3 >$	0.0363	0.0347

Discussion of the Lamb shift / electron scattering discrepancy

Zemach-Moments:

- A. C. Zemach, *Proton Structure and the Hyperfine Shift in Hydrogen*, Phys. Rev. **104**, 1771 (1956).

$$< r^3 >_{(2)} = \int_0^\infty \frac{dq}{q^4} \left(G_E^2(q^2) - 1 + q^2 < r^2 >_p /3 \right)$$

$$< r^3 >_{(2)} = 2.27\,\mathrm{fm}^3 \qquad \longrightarrow \qquad r_p = 0.84184(67)\,\mathrm{fm}$$

Discussion of the Lamb shift / electron scattering discrepancy

Zemach-Moments:

- A. C. Zemach, *Proton Structure and the Hyperfine Shift in Hydrogen*, Phys. Rev. **104**, 1771 (1956).

$$< r^3 >_{(2)} = \int_0^\infty \frac{dq}{q^4} \left(G_E^2(q^2) - 1 + q^2 < r^2 >_p /3 \right)$$

$$< r^3 >_{(2)} = 2.27\,\mathrm{fm}^3 \quad \longrightarrow \quad r_p = 0.84184(67)\,\mathrm{fm}$$
$$< r^3 >_{(2)} = 2.85(8)\,\mathrm{fm}^3 \quad \longrightarrow \quad r_p = 0.84245(67)\,\mathrm{fm}$$

- M.O.D., J.C. Bernauer, and Th. Walcher, *The RMS Charge Radius of the Proton and Zemach Moments*, in Press doi:10.1016/j.physletb.2010.12.067, arXiv:1011.1861.

2S – 2P splitting in muonic hydrogen

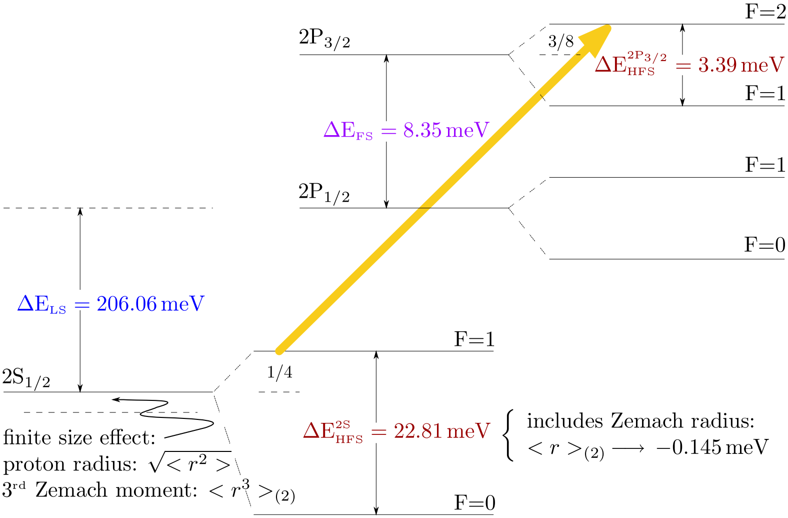

De Rújula's toy model

- A. De Rújula, "QED is not endangered by the proton's size", Phys. Lett. **B693**, 555 (2010).
- **Sum of "single pole" and "dipole"**

$$\rho_{\text{Proton}}(r) = \frac{1}{D}\left[\frac{M^4 e^{-Mr}\cos^2(\theta)}{4\pi r} + \frac{m^5 e^{-mr}\sin^2(\theta)}{8\pi}\right]$$
$$D \equiv M^2\cos^2(\theta) + m^2\sin^2(\theta)$$

using $M = 0.750\,\mathrm{GeV/c^2}$, $m = 0.020\,\mathrm{GeV/c^2}$, and $sin^2(\theta) = 0.3$ and

$$\rho_{(2)}(r) = \int d^3r_2\,\rho_{\mathrm{charge}}(|\vec{r}-\vec{r_2}|)\,\rho_{\mathrm{charge}}(r_2)$$

we get the **third Zemach moment**:

$$\langle r^3\rangle_{(2)} = \int d^3r\,r^3\rho_{(2)}(r) = 36.2\,\mathrm{fm}^3$$

We put $\langle r^3\rangle_{(2)} = 36.2\,\mathrm{fm}^3$ in the Lamb shift formular:

$$L^{5th}[\langle r^2\rangle, \langle r^3\rangle_{(2)}] =$$

$$\left(209.9779(49) - 5.2262\,\frac{\langle r^2\rangle}{\mathrm{fm}^2} + 0.00913\,\frac{\langle r^3\rangle_{(2)}}{\mathrm{fm}^3}\right)\mathrm{meV}$$

and get $r_p = 0.878\,\mathrm{fm}$

We put $\langle r^3 \rangle_{(2)} = 36.2\,\mathrm{fm}^3$ in the Lamb shift formular:

$$L^{5th}[\langle r^2 \rangle, \langle r^3 \rangle_{(2)}] = \left(209.9779(49) - 5.2262\,\frac{\langle r^2 \rangle}{\mathrm{fm}^2} + 0.00913\,\frac{\langle r^3 \rangle_{(2)}}{\mathrm{fm}^3}\right)\mathrm{meV}$$

and get $r_p = 0.878\,\mathrm{fm}$

problem solved

De Rújula's toy model – is excluded by experiment

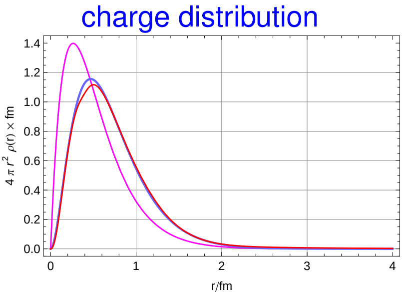

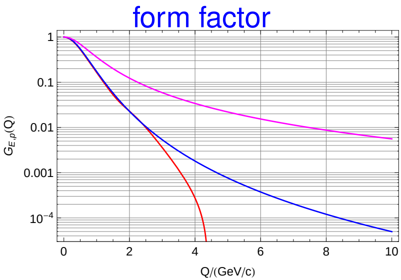

- De Rújula's toy model
- standard dipole
- Bernauer-Arrington fit assembly

Speculation about the discrepancy

- Reminder: The muon g-2 experiment has a $2-3\sigma$ discrepancy. Hadronic corrections may provide an explanation.
- The main contribution to the **Lamb shift** in . . .

Speculation about the discrepancy

- Reminder: The muon g-2 experiment has a $2-3\sigma$ discrepancy. Hadronic corrections may provide an explanation.
- The main contribution to the **Lamb shift** in ...

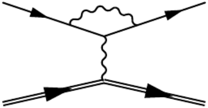

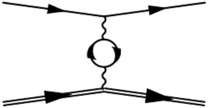

	'electronic' hydrogen	muonic hydrogen
vertex and self-energy	$1011.41\,\mathrm{MHz}$	
vacuum polarization	$-27.13\,\mathrm{MHz}$	$-205.028\,\mathrm{meV}$
anom. magn. moment	$67.82\,\mathrm{MHz}$	
+ higher order		
theoretical value	$1057.864(14)\,\mathrm{MHz}$	$-206.057\,\mathrm{meV}$
experimental value	$1057.862(20)\,\mathrm{MHz}$	$\Delta : 0.341\,\mathrm{meV}$

Speculation about the discrepancy

- If we assign the difference of the two determinations of the radius of 0.038 fm fully to the energy difference of the 2S-2P point nucleus Lamb shift we get a shift of $-0.341\,\mathrm{meV}$
- The mass of an electrically charged particle-antiparticle pair producing such a Lamb shift would be 23 MeV.
- No free particle with this mass is known.

Speculation about the discrepancy

- If we assign the difference of the two determinations of the radius of 0.038 fm fully to the energy difference of the 2S-2P point nucleus Lamb shift we get a shift of $-0.341\,\mathrm{meV}$
- The mass of an electrically charged particle-antiparticle pair producing such a Lamb shift would be 23 MeV.
- No free particle with this mass is known.
- However, quantum mechanics requests fluctuations of quarks-antiquarks also in the Coulomb field.
- Considering the small energy scales in muonic hydrogen, 23 MeV does not unreasonably compare to the current quark masses $m_{up} \approx 3\,\mathrm{MeV/c^2}$ and $m_{down} \approx 2m_{up}$ at the $2\,\mathrm{GeV}$ scale.
- If true, one could revert the interpretation of the muonic hydrogen experiment if we assume that the QED calculations are sufficiently exact. By inserting the precise radius from the electronic experiments and the safe Zemach moments, one can determine the polarisation in the Coulomb field by quark loops or other hadronic corrections at a very low Q2 scale.

Conclusion – Part II

- High precision form factors from MAMI provide constraints for the charge distribution of the proton.
- Standard dipole approximation is not sufficient for correction of the muonic hydrogen Lamb shift.
- The proton size discrepancy is between the Lamb shift of muonic hydrogen and every ”electronic” determination.
- Possible explanation for the discrepancy: Coupling of QED and QCD (”quark loops”).
- M.O.D., J.C. Bernauer, and Th. Walcher, *The RMS Charge Radius of the Proton and Zemach Moments*, in Press doi:10.1016/j.physletb.2010.12.067, arXiv:1011.1861.

Supported by the “Deutsche Forschungsgemeinschaft (DFG)” with a “Sonderforschungsbereich (SFB443)”.

Outlook: Initial state radiation

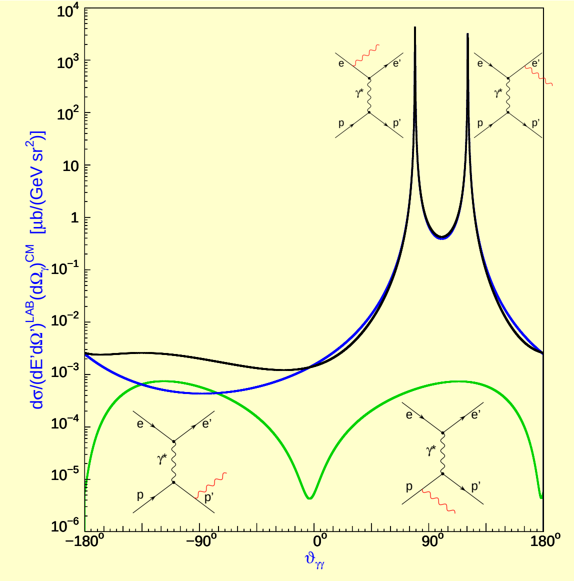

Outlook: Initial state radiation

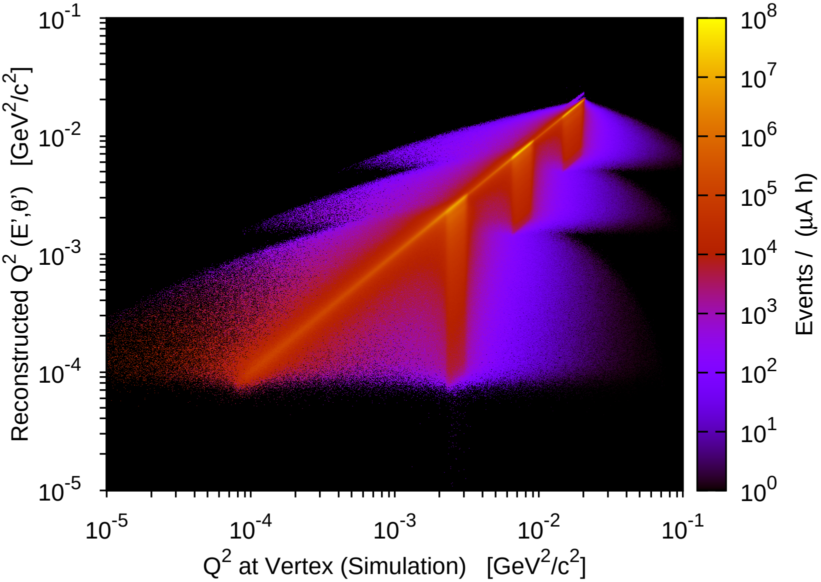

Backup

Discussion of the Lamb shift / electron scattering discrepancy

The following tables are taken from the 'QED supplement' published in *Nature* **466**, 213-216 (8 July 2010).
'All known radius-independent contributions' and 'all relevant radius-dependent contributions' to the Lamb shift in μp from different authors are listed.

Discussion of the Lamb shift / electron scattering discrepancy

#	Contribution	Ref.	Our selection Value	Our selection Unc.	Pachucki[1–3] Value	Pachucki[1–3] Unc.	Borie[5] Value	Borie[5] Unc.
1	NR One loop electron VP	1,2			205.0074			
2	Relativistic correction (corrected)	1–3,5			0.0169			
3	Relativistic one loop VP	5	205.0282				205.0282	
4	NR two-loop electron VP	5,14	1.5081		1.5079		1.5081	
5	Polarization insertion in two Coulomb lines	1,2,5	0.1509		0.1509		0.1510	
6	NR three-loop electron VP	11	0.00529					
7	Polarisation insertion in two and three Coulomb lines (corrected)	11,12	0.00223					
8	Three-loop VP (total, uncorrected)				0.0076		0.00761	
9	Wichmann-Kroll	5,15,16	−0.00103				−0.00103	
10	Light by light electron loop contribution (Virtual Delbrück scattering)	6	0.00135	0.00135			0.00135	0.00015
11	Radiative photon and electron polarization in the Coulomb line $\alpha^2(Z\alpha)^4$	1,2	−0.00500	0.0010	−0.006	0.001	−0.005	
12	Electron loop in the radiative photon of order $\alpha^2(Z\alpha)^4$	17–19	−0.00150					
13	Mixed electron and muon loops	20	0.00007				0.00007	
14	Hadronic polarization $\alpha(Z\alpha)^4 m_r$	21–23	0.01077	0.00038	0.0113	0.0003	0.011	0.002
15	Hadronic polarization $\alpha(Z\alpha)^5 m_r$	22,23	0.000047					
16	Hadronic polarization in the radiative photon $\alpha^2(Z\alpha)^4 m_r$	22,23	−0.000015					
17	Recoil contribution	24	0.05750		0.0575		0.0575	
18	Recoil finite size	5	0.01300	0.001			0.013	0.001
19	Recoil correction to VP	5	−0.00410				−0.0041	
20	Radiative corrections of order $\alpha^n(Z\alpha)^k m_r$	2,7	−0.66770		−0.6677		−0.66788	
21	Muon Lamb shift 4th order	5	−0.00169				−0.00169	
22	Recoil corrections of order $\alpha(Z\alpha)^5 \frac{m}{M} m_r$	2,5–7	−0.04497		−0.045		−0.04497	
23	Recoil of order α^6	2	0.00030		0.0003			
24	Radiative recoil corrections of order $\alpha(Z\alpha)^n \frac{m}{M} m_r$	1,2,7	−0.00960		−0.0099		−0.0096	
25	Nuclear structure correction of order $(Z\alpha)^5$ (Proton polarizability contribution)	2,5,22,25	0.015	0.004	0.012	0.002	0.015	0.004
26	Polarization operator induced correction to nuclear polarizability $\alpha(Z\alpha)^5 m_r$	23	0.00019					
27	Radiative photon induced correction to nuclear polarizability $\alpha(Z\alpha)^5 m_r$	23	−0.00001					
	Sum		206.0573	0.0045	206.0432	0.0023	206.05856	0.0046

Discussion of the Lamb shift / electron scattering discrepancy

#	Contribution		Our selection		Pachucki[1–3]		Borie[5]	
		Ref.	Value	Unc.	Value	Unc.	Value	Unc.
1	NR One loop electron VP	1,2			205.0074			
2	Relativistic correction (corrected)	1–3,5			0.0169			
3	Relativistic one loop VP	5	205.0282				205.0282	
4	NR two-loop electron VP	5,14	1.5081		1.5079		1.5081	
5	Polarization insertion in two Coulomb lines	1,2,5	0.1509		0.1509		0.1510	
6	NR three-loop electron VP	11	0.00529					
7	Polarisation insertion in two and three Coulomb lines (corrected)	11,12	0.00223					
8	Three-loop VP (total, uncorrected)				0.0076		0.00761	
9	Wichmann-Kroll	5,15,16	−0.00103				−0.00103	
10	Light by light electron loop contribution (Virtual Delbrück scattering)	6	0.00135	0.00135			0.00135	0.00015
11	Radiative photon and electron polarization in the Coulomb line $\alpha^2(Z\alpha)^4$	1,2	−0.00500	0.0010	−0.006	0.001	−0.005	
12	Electron loop in the radiative photon of order $\alpha^2(Z\alpha)^4$	17–19	−0.00150					
13	Mixed electron and muon loops	20	0.00007				0.00007	
14	Hadronic polarization $\alpha(Z\alpha)^4 m_r$	21–23	0.01077	0.00038	0.0113	0.0003	0.011	0.002

Discussion of the Lamb shift / electron scattering discrepancy

15	Hadronic polarization $\alpha(Z\alpha)^5 m_r$	22,23	0.000047					
16	Hadronic polarization in the radiative photon $\alpha^2(Z\alpha)^4 m_r$	22,23	−0.000015					
17	Recoil contribution	24	0.05750		0.0575		0.0575	
18	Recoil finite size	5	0.01300	0.001			0.013	0.001
19	Recoil correction to VP	5	−0.00410				−0.0041	
20	Radiative corrections of order $\alpha^n(Z\alpha)^k m_r$	2,7	−0.66770		−0.6677		−0.66788	
21	Muon Lamb shift 4th order	5	−0.00169				−0.00169	
22	Recoil corrections of order $\alpha(Z\alpha)^5 \frac{m}{M} m_r$	2,5–7	−0.04497		−0.045		−0.04497	
23	Recoil of order α^6	2	0.00030		0.0003			
24	Radiative recoil corrections of order $\alpha(Z\alpha)^n \frac{m}{M} m_r$	1,2,7	−0.00960		−0.0099		−0.0096	
25	Nuclear structure correction of order $(Z\alpha)^5$ (Proton polarizability contribution)	2,5,22,25	0.015	0.004	0.012	0.002	0.015	0.004
26	Polarization operator induced correction to nuclear polarizability $\alpha(Z\alpha)^5 m_r$	23	0.00019					
27	Radiative photon induced correction to nuclear polarizability $\alpha(Z\alpha)^5 m_r$	23	−0.00001					
	Sum		206.0573	0.0045	206.0432	0.0023	206.05856	0.0046

Discussion of the Lamb shift / electron scattering discrepancy

$$\Delta E = 209.9779(49) - 5.2262\, r_p^2 + 0.0347\, r_p^3$$

Values are in meV and radii in fm.

Contribution	Ref.	our selection		Pachucki[2]	Borie[5]
Leading nuclear size contribution	[26]	−5.19745	$< r_p^2 >$	−5.1974	−5.1971
Radiative corrections to nuclear finite size effect	[2,26]	−0.0275	$< r_p^2 >$	−0.0282	−0.0273
Nuclear size correction of order $(Z\alpha)^6 < r_p^2 >$	[1,27–29]	−0.001243	$< r_p^2 >$		
Total $< r_p^2 >$ contribution		−5.22619	$< r_p^2 >$	−5.2256	−5.2244
Nuclear size correction of order $(Z\alpha)^5$	[1,2]	0.0347	$< r_p^3 >$	0.0363	0.0347

Data taking periods

	August 2006	November 2006	May 2007
Duration	10 days	11 days	17 days
without setup/calibration	8 days	9 days	11 days
Energies	575, 850 MeV	180, 720 MeV	315, 450 MeV
Setting changes	152	173	202
data taking time	3.3 days	4.3 days	5.3 days
Average time per setting	31 min	35 min	38 min
Overhead per setting	44 min	40 min	40 min

- Overhead includes angle changes, momentum changes and down times.
- Average time for ”angle only” setting changes: 10 min.

Form factor results

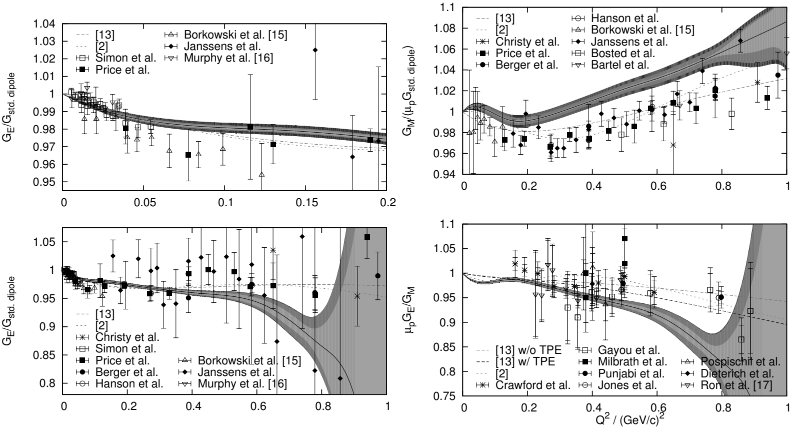

Backup

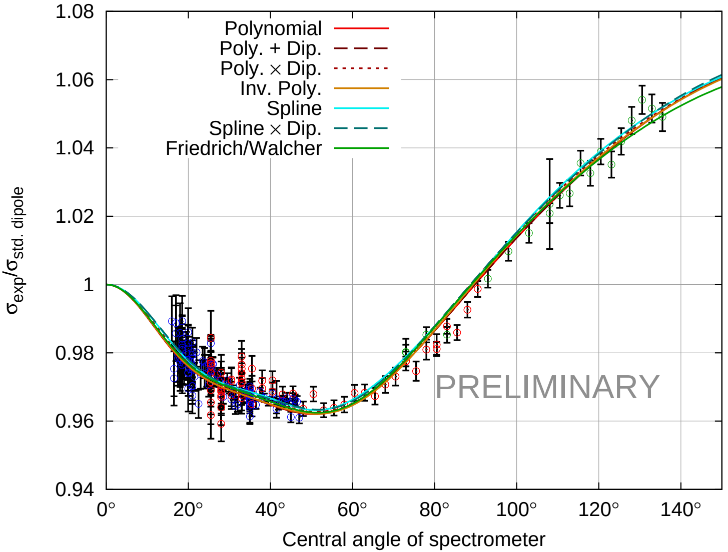

Polynomial
Poly. + Dip.
Poly. × Dip.
Inv. Poly.
Spline
Spline × Dip.
Friedrich/Walcher
PRELIMINARY
$\sigma_{exp}/\sigma_{std.\ dipole}$
1.08
1.06
1.04
1.02
1
0.98
0.96
0.94
0°
20°
40°
60°
80°
100°
120°
140°
Central angle of spectrometer

Cross sections: 315 MeV

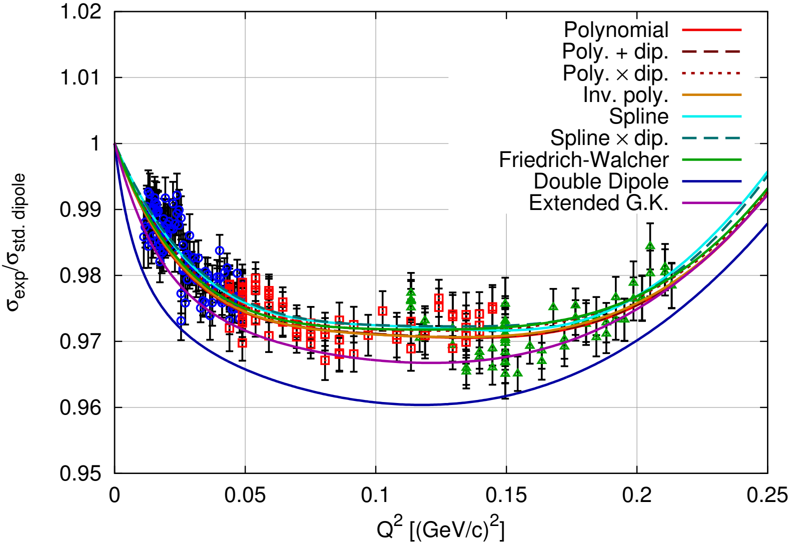

Cross sections: 450 MeV

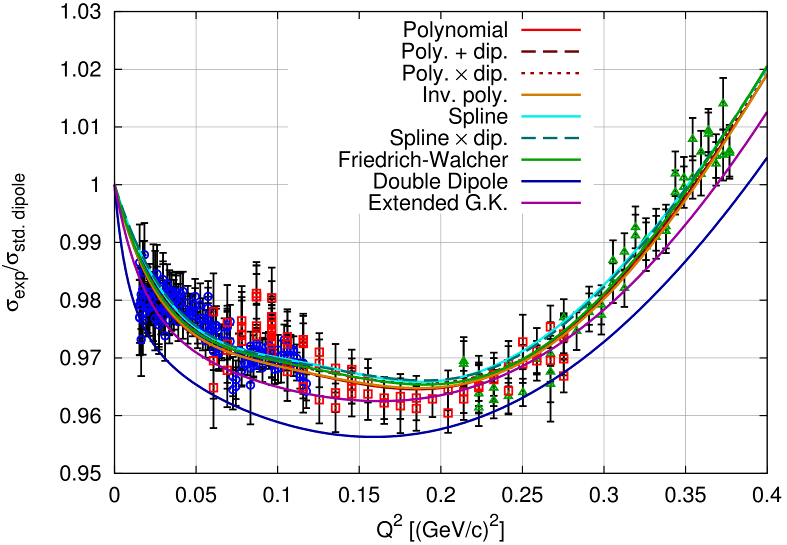

Cross sections: 585 MeV

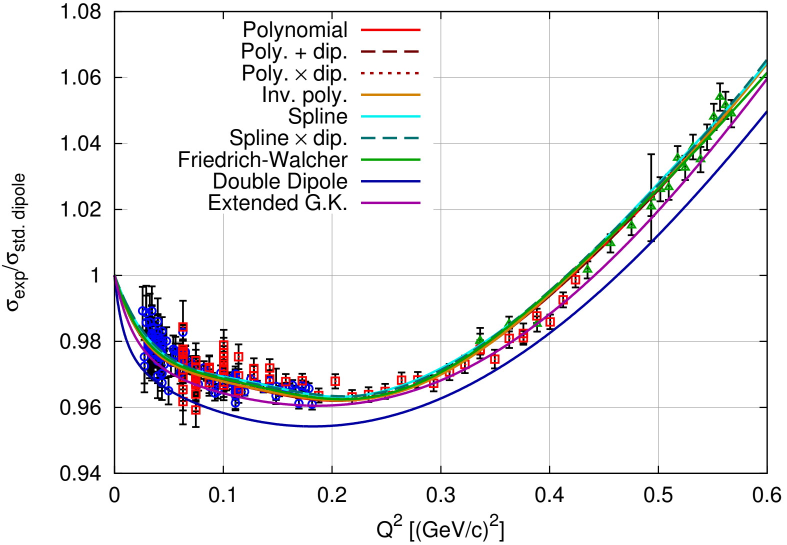

Cross sections: 720 MeV

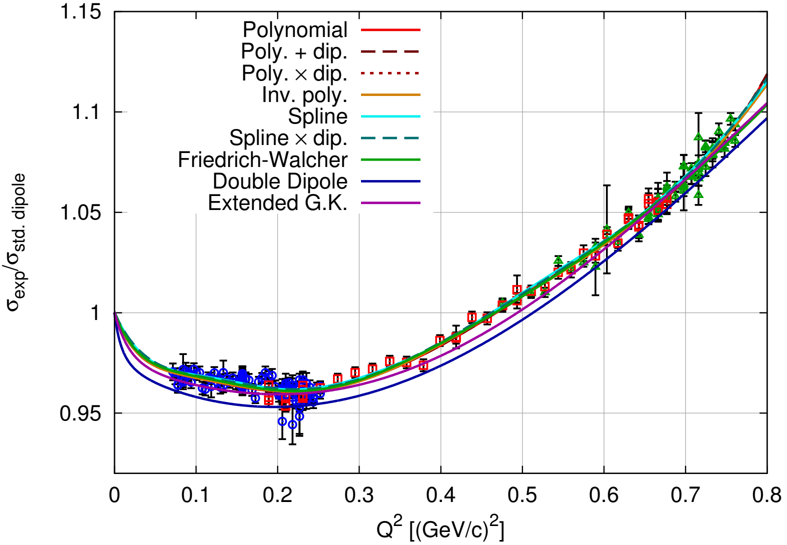

Cross sections: 855 MeV

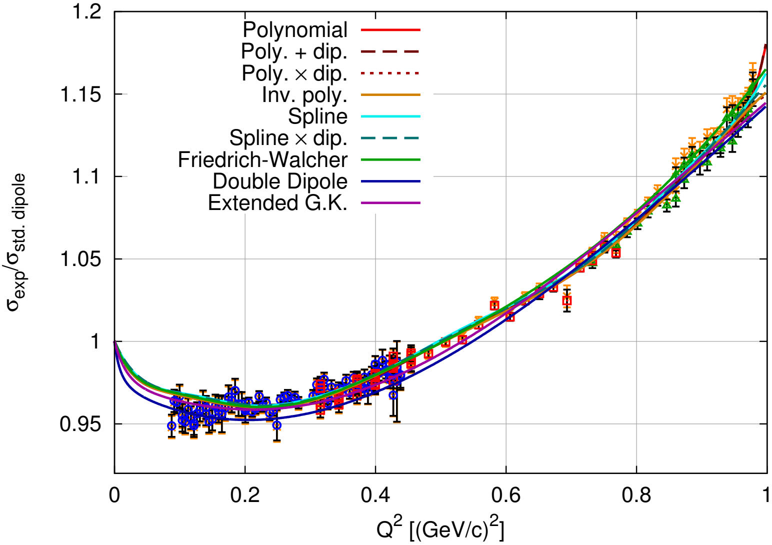

Rosenbluth separation

$$Q^2 = 0.15\ (\text{GeV}/c)^2$$

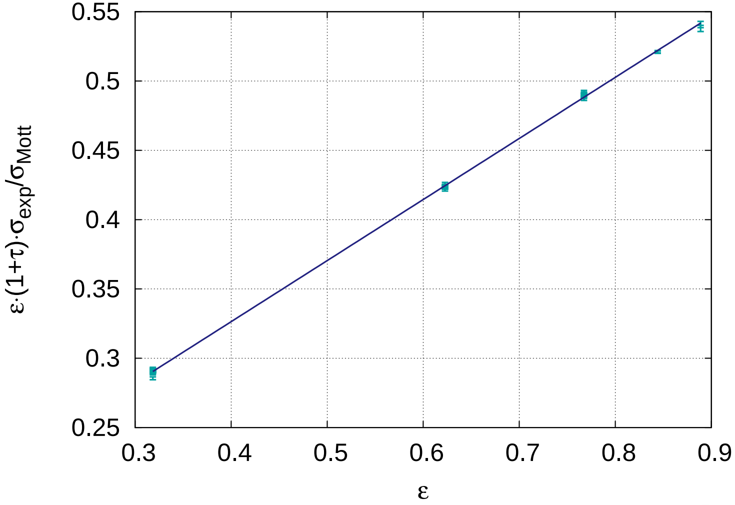

. . . more . . .

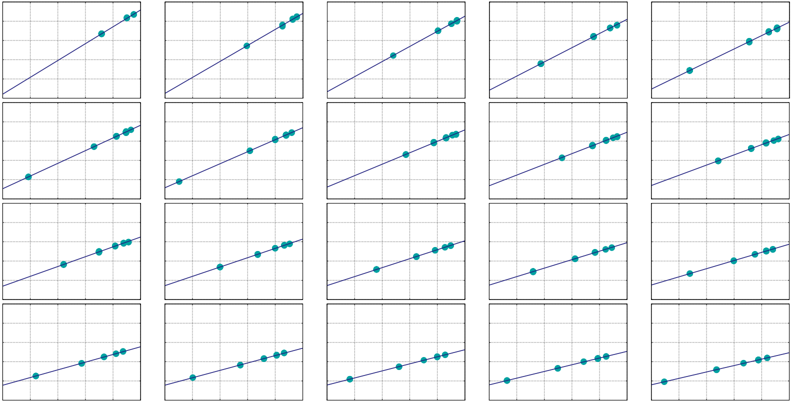

. . . and more . . .

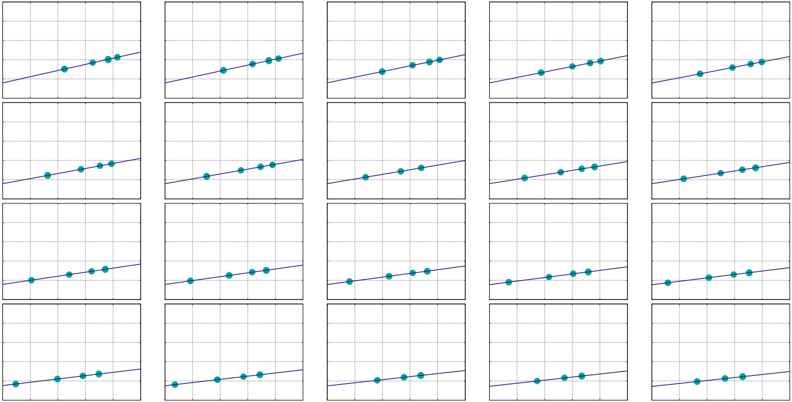

. . . and even more

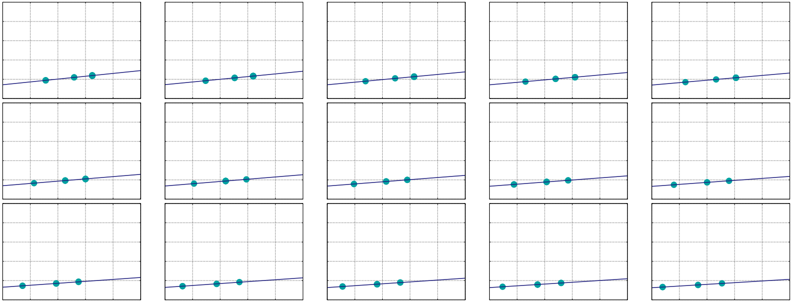

Comparison: Rosenbluth vs. Spline fit

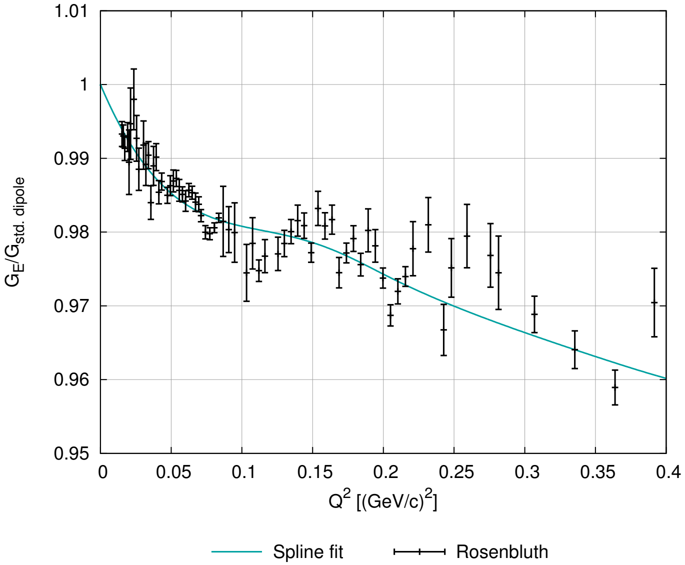

Model dependence of radius extraction

Check extraction of radii with Monte-Carlo data:

- Monte-Carlo data from given parametrization (known radii!)
- Error distribution of this simulated data according to errors from real data
- Fit with different models

Assumption: $\pm 5\%$ normalization error (per spectrometer/energy)

Model dependence: Charge Radius

Analysis of simulated pseudo data

Input		Analysis							
		Dipole	Dbl-D.	Poly.	P.+D.	P.×D.	Spline	S.×D.	F./W.
Std. dipole	811	0±1	0±1	0±3	0±3	0±4	0±5	0±7	0±1
Arrington 07	878	−18±1	3±3	−3±3	−2±3	−1±4	−4±5	−1±6	−2±3
Arr. 03 (P)	829	29±1	10±1	1±3	1±3	0±4	−1±5	0±6	2±6
Arr. 03 (R)	868	−9±1	0±2	0±3	0±3	0±4	−3±5	0±6	−1±3
FW	860	−4±1	31±14	−1±3	−1±3	1±4	0±5	0±6	0±3

Spline fit + error band

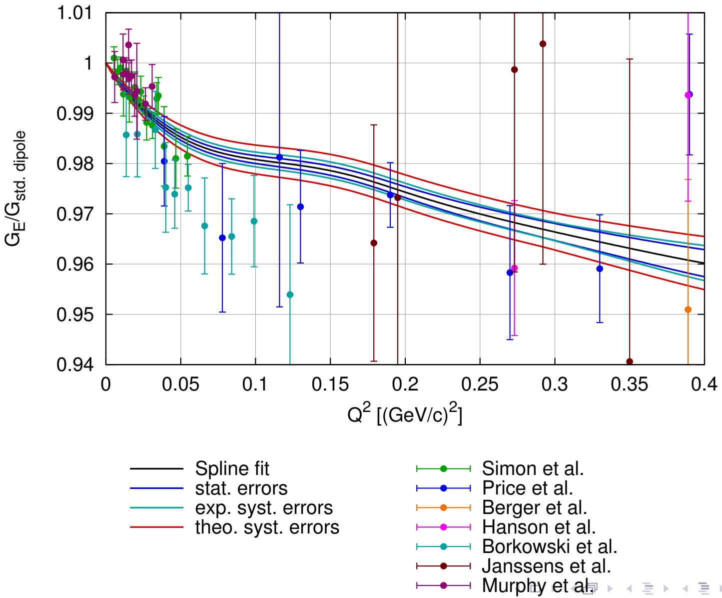

Spline fit + error band

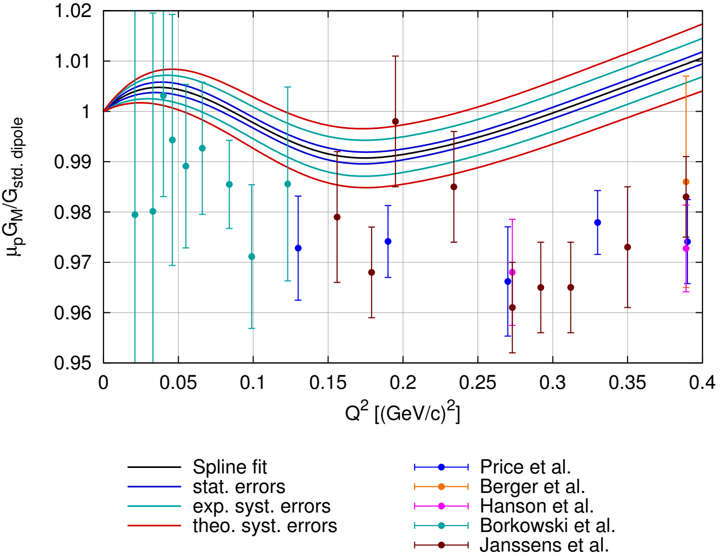

The cryogenic target system

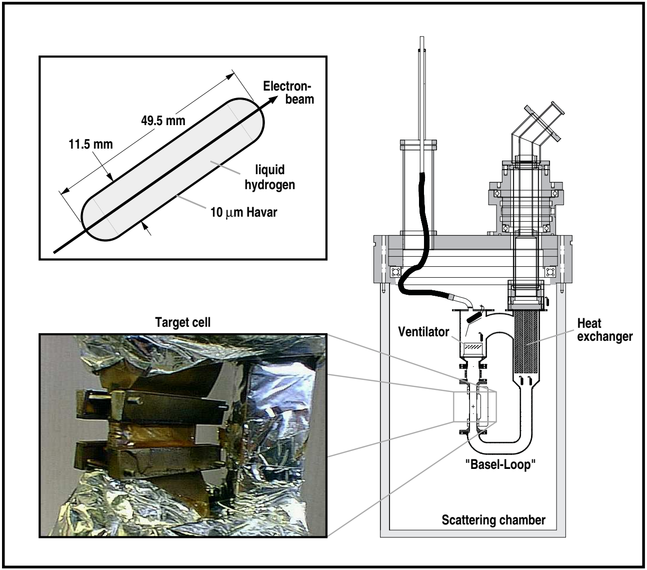

Model dependence: Magnetic Radius

Analysis of simulated pseudo data

Input		Analysis							
		Dipole	Dbl-D.	Poly.	P.+D.	P.$\times$D.	Spline	S.$\times$D.	F./W.
Std. dipole	811	0 ± 1	0 ± 1	-1 ± 7	0 ± 7	0 ± 10	2 ± 14	1 ± 18	0 ± 1
Arrington 07	858	-55 ± 1	4 ± 4	-5 ± 6	-4 ± 6	-1 ± 9	2 ± 13	0 ± 17	-10 ± 4
Arr. 03 (P)	837	-33 ± 1	12 ± 3	-1 ± 7	0 ± 7	0 ± 9	2 ± 13	0 ± 19	-5 ± 5
Arr. 03 (R)	863	-52 ± 1	2 ± 4	-4 ± 6	-3 ± 6	0 ± 9	3 ± 13	0 ± 17	-8 ± 4
FW	805	4 ± 1	49 ± 2	0 ± 7	1 ± 7	-1 ± 10	1 ± 13	-1 ± 18	-1 ± 4